Study of radiation effects on Er^{3+}-doped nanoparticles germano-silica fibers

B. Hari Babu, Nadege Ollier, Inna Savelli, Hicham El Hamzaoui, A. Pastouret, Bertrand Poumellec, Mohamed Bouazaoui, Laurent Bigot, Matthieu Lancry

Study of Radiation Effects on Er^{3+}-Doped Nanoparticles Germano-Silica Fibers

B. Hari Babu, Nadege Ollier, Inna Savelli, Hicham El Hamzaoui, A. Pastouret, Bertrand Poumellec, Mohamed Bouazaoui, Laurent Bigot, and Matthieu Lancry

***Abstract*—The main goal of the present work is to study the impact of Er–SiO_2 and Er–Al_2O_3 nanoparticles on the radiation induced defects in germano-silica optical fibers with Al/Ge ranges over 0.1–150. These fibers are prepared by a modified chemical vapor deposition technique and are characterized by optical absorption and electron paramagnetic resonance spectroscopy. High amount of Ge, Er–SiO_2 nanoparticles-derived optical fibers exhibit lower radiation induced attenuation than those with a low Ge content undoped or doped with Al_2O_3 nanoparticles. Furthermore, the behavior of point defects namely GeE', Ge(1), SiE', nonbridging oxygen hole centers, and H(1) is reported according to the Al/Ge ratio. In contrast to the optical fiber preforms, no Al-related defects are found in the optical fibers. Therefore, the results evidence the strong radiation tolerance by the virtue of the nanoparticle doping, which is enabling technology for the development of the photonic and space applications in the radiation fields.**

***Index Terms*—Electron paramagnetic resonance, erbium-doped optical amplifiers, germano-silica fibers, oxide nanoparticles, radiation resistance, γ-rays.**

I. Introduction

OVER the last twenty years, the Er^{3+} doped silica based fibers become a key element to the high volume market due to its exceptional usage as optical amplifiers for ground optical communication systems and fiber lasers [1]–[4]. Moreover, the nanoparticles incorporated into the Er^{3+} doped silica glasses and fibers resulting improvement in the homogeneity of the Er^{3+} ions in the host, changes in the environment led to the enhancement of the near infrared luminescence ($\sim$1.53 μm) as well as an "eye-safer" wavelength ($\lambda > 1400$ nm), where an optical energy is not an attentive on the retina [1], [4]. In addition, the silica based optical fiber applications are extended for the military and satellite communications in the harsh environment [5]–[7]. Many studies so far have been devoted to the characterization and fabrication for the radiation response of silica glass and fibers with single and codopants (Ge, P, Ce, Yb^{3+} and Al_2O_3 with Er^{3+}) [1]–[8]. However, the radiodarkening phenomena of optical fibers are of a particular concern as exposed to ionizing radiation and are a detrimental process since it affects both transmission losses, optical amplifier gain and its flatness [2], [3]–[10]. This excess loss is also known as radiation induced attenuation (RIA) that can arise from the light absorption taken place by the radiation induced color centers at the pump (0.98 μm) and signal (1.53 μm) wavelengths respectively [2], [3], [5]–[12]. An effective strategy could be improved the radiation hardening of optical fibers through different approaches, namely glass network formers and modifiers (Ge, P, Ce and F) doping [2], [8], [11], hydrogenation coating [2], [13], [14], hole-assisted carbon coating [15], fictive temperature [16] and more recently by means of nanoparticles doping process [17], [18].

Research on the erbium doped fiber amplifiers (EDFAs) brought into the light strong sensitivity to radiations of these active fibers in comparison to the pure-silica-core or germano-silicate host fibers [19], [20]. The radiation sensitivity is not only caused by the Er^{3+} ion doping, but also the co-dopants that facilitates the Er^{3+} incorporation into the silica network. Now, it is perfectly clear that Al-related defects (AlOHC and AlE') explain the high RIA-levels in Al-doped glasses and optical fibers under ionizing radiation [2], [5], [12]. The potential benefit of the nanoparticles doping process has been developed by Draka and it is pointed out in the frame of radiation hardened erbium doped fiber amplifiers (EDFAs). Recently, Thomas et al. established strongest gain-degradation for the optical amplifiers using the standard technology based fibers with the highest aluminium concentration, while the lowest gain-degradation (-0.5 dB) are noticed for the silica nanoparticles based fibers, without aluminium traces [17], [18]. Therefore, this work demonstrates for the first time the feasibility of radiation resistant single-channel EDFAs designed for space applications.

Manuscript received April 13, 2016; revised July 28, 2016; accepted August 7, 2016. Date of publication August 9, 2016; date of current version October 13, 2016. The work was supported in part by the French National Research Agency through the NANOFIBER project under Grant ANR-12-RMNP-0019, in part by the Nord-Pas de Calais Regional Council, in part by the FEDER through the "Contrat de Projets Etat Region (CPER) 2007-2013", in part by the "Campus Intelligence Ambiante", in part by the FLUX Equipex Project under Grant ANR-11-EQPX-0017, and in part by the Labex CEMPI under Grant ANR-11-LABX-0007.

B. Hari Babu is with the Laboratoire des Solides Irradiés, CNRS, CEA, Ecole Polytechnique, Université Paris Saclay, Palaiseau 91128, France, and also with the Institut de Chimie Moléculaire et des Matériaux d'Orsay, SP2M, CNRS-Université Paris Sud, Université Paris Saclay, Orsay 91405, France (e-mail: hariphy2012@gmail.com).

N. Ollier is with the Laboratoire des Solides Irradiés, CNRS, CEA, Ecole Polytechnique, Université Paris Saclay, Palaiseau 91128, France (e-mail: nadege.ollier@polytechnique.edu).

I. Savelii, H. El Hamzaoui, M. Bouazaoui, and L. Bigot are with the Laboratoire de Physique des Lasers, Atomes et Molécules, Institut de Recherche sur les Composants logiciels et matériels pour l'Information et la Communication Avancée, CNRS-Universite Lille 1, Villeneuve-d'Ascq 59650, France (e-mail: Inna.Savelii@univ-lille1.fr; Hicham.Elhamzaoui@phlam.univ-lille1.fr; Mohamed.Bouazaoui@univ-lille1.fr; laurent.bigot@univ-lille1.fr).

B. Poumellec and M. Lancry are with the Institut de Chimie Moléculaire et des Matériaux d'Orsay, SP2M, CNRS-Université Paris Sud, Université Paris Saclay, Orsay 91405, France (e-mail: bertrand.poumellec@u-psud.fr; Matthieu.Lancry@u-psud.fr).

A. Pastouret is with Draka Comteq France SAS, Parc des Industries Artois Flandres, Haisnes Cedex 62138, France (e-mail: Alain.PASTOURET@prysmiangroup.com).

Color versions of one or more of the figures in this paper are available online at http://ieeexplore.ieee.org.

Digital Object Identifier 10.1109/JLT.2016.2599173

TABLE I
FIBER LABELS, COMPOSITION (WT.%), Er^{3+} LOSS AT 980 NM (α) DB/M, NANOPARTICLE SIZE (NP), CORE DIAMETER (ϕ) ARE GIVEN FOR THE STUDIED Er^{3+} DOPED GERMANO-SILICA FIBERS

Fiber Labels	Ge	Al	Al/Ge	α	Er^{3+}	NP	Φ (μm)
SiNP	24.3	0.05	0.002	12.0	0.05	Si-25	2.87
Al/Ge0.012	25	0.3	0.012	4.69	0.019	–	2.58
Al/Ge0	20	–	–	–	–	–	5.31
AlNP-Al/Ge0.013	22.5	0.3	0.013	9.6	0.04	Al-25	3.19
AlNP-Al/Ge0.705	4.4	3.1	0.705	5.36	0.022	Al-25	4.92
AlNP-Al/Ge0.854	2.6	2.22	0.854	10.85	0.045	Al-25	4.57
AlNP-Al/Ge6	0.75	4.5	6.0	23.2	0.097	Al-25	4.57
AlNP-Al/Ge60	0.05	3.0	60	19.0	0.079	Al-05	5.63
Al/Ge120	0.05	6.0	120	3.56	0.015	–	3.27
Al/Ge150	0.05	7.5	150	22	0.092	–	4.31

The main objective of this paper is to report on the γ-radiation resistance of optical fibers doped by alumina or silica nanoparticles containing Er^{3+} ions, after irradiation dose of 5.9 kGy. The nanoparticles have been synthesized and then incorporated by the solution doping inside the soot core fabricated, using the Modified Chemical Vapor Deposition (MCVD) technique. The generation of point defects in γ-irradiated optical fibers are studied systematically as a function of the Al/Ge ratio in the presence of nanoparticles. The purpose of this work is to reduce the defect concentration and the RIA through the nanoparticle doping and host variations.

II. EXPERIMENTAL DETAILS

A suspension of Er^{3+}-doped Al_2O_3 or SiO_2 nanoparticle precursors were prepared using the co-precipitation method [4], then incorporated within the MCVD optical fiber preforms through a classical liquid doping technique. The Er^{3+} doped oxide NPs have been manufactured by the soft chemical synthesis. Afterwards, they have been dispersed in a stable suspension. By this method five types of Er-doped NPs with a diameter of 25 nm and different specific NP matrix have been prepared. The different matrix compositions are as follows: SiO_2 with a Si/Er molar ratio of 200, Al_2O_3 with two different Al/Er molar ratios (200 and 30), and Al_2O_3 (Er free). Additionally, another smaller NP type with Al/Er ratio equal to 200 and a diameter of 5 nm has been prepared. After dehydration, collapsing and over cladding, the fabricated preforms have been drawn into conventional single mode fibers. For comparison, a standard Er^{3+}-doped optical preforms with similar Er concentration is fabricated by soaking Er^{3+} salts in a silica-based core layer manufactured by MCVD and codoped with Ge and Al. This sample is labelled as BEF (Basic Erbium Fiber). Two sets of fibers are studied according to the Al content and the Al/Ge ratio, their chemical composition and characteristics are presented in Table. I. All the fibers were irradiated with 1.25 MeV γ-rays from ^{60}Co radioactive source, at room temperature, in the Institut de Radioprotection et de Sureté Nucléaire (IRSN, Fontenay-aux-Roses, France). The net irradiation dose of 5.9 kGy is achieved with a dose rate of 14 Gy/min.

The absorption measurements of optical fibers were carried out by using a standard cut-back technique with Photon Kinetics' 2200 Fiber Analysis. The electron paramagnetic resonance (EPR) spectrometer is performed using Bruker X-band EMX spectrometer at X-band frequency (9.868 GHz) with a modulation of 100 kHz for analyzing point defect generation. The resultant EPR spectra are normalized by the gain and fiber core volume in order to distinguish the Ge, Al-related defect concentrations precisely. Concerning H(I) defects, the EPR spectra are normalized by the gain and mass of fibers. All experiments were done at room temperature (RT) only.

The optical absorption coefficient was calculated from the ratio of optical density to the difference of the length of the fibers. The RIA spectra of studied fibers were calculated as the difference of the pre- and post-irradiation spectra of fibers and their estimated error should be around $\pm$ 4%. Moreover, it was impossible to measure optical loss at 0.98 μm and 1.53 μm of the Er^{3+} absorption bands since the absorption was too large. Thus, RIA spectra were interpolated in this spectral region [2]. Similarly, the EPR spectra were normalized by the fiber core volume and attenuator's gain. The core diameter of the fibers was calculated from the Ge and Al profiles obtained from the electron probe micro-analysis (EPMA). The estimated error in the EPR spectra which was around $\pm$ 6.0%.

III. RESULTS

A. Optical Attenuation

The attenuation spectra of Er^{3+}-doped germano-silica fibers are recorded in the near infrared spectral range of 650–1750 nm, before γ-ray irradiation. They exhibit two significant absorption bands located at around 980 nm and 1530 nm, which are commonly referred to the electronic transitions from a ground state ($^4I_{15/2}$) to the respective excited states $^4I_J (J = 11/2, 13/2)$ of Er^{3+} ions [21]. Before γ-irradiation, the background attenuation of all fibers is found to be smaller than $\sim$0.005 dB/m.

B. Radiation Induced Attenuation

Radiation induced attenuation (RIA) spectra of Er^{3+} doped SiO_2 and Al_2O_3-nanoparticles germano-silica fibers with different Al/Ge ratio (0.002–0.013) are shown in Fig. 1(a). Let us first consider, the Al free and Al codoped germano-silica fibers with a concentration of Al_2O_3 (typically $\leq$ 0.3 wt.%). For a pure germano-silica optical fiber (Al/Ge0) without nanoparticles and Er, it can be seen that the RIA level is nearly 0.14 dB/m at 1.53 μm after 5.9 kGy γ-irradiation.

Secondly, the SiNP fiber displays the RIA level, which seems to be slightly lower as compared to the Al/Ge0 fiber. This demonstrates no significant impact of Er when it is introduced in the form of Er_2O_3-SiO_2 nanoparticles in the glass matrix with Al_2O_3 content of 0.05 wt.%. Based on the previous work reported in the literature, the SiNP fiber establishes lower RIA ($\sim$0.03 dB/m at 1.53 μm) in the present case [2], [3], [12]. This is likely due to the fact that erbium and small amount of aluminum oxide was introduced within SiO_2 nanoparticles when compared to the standard MCVD process [2], [3], [12].

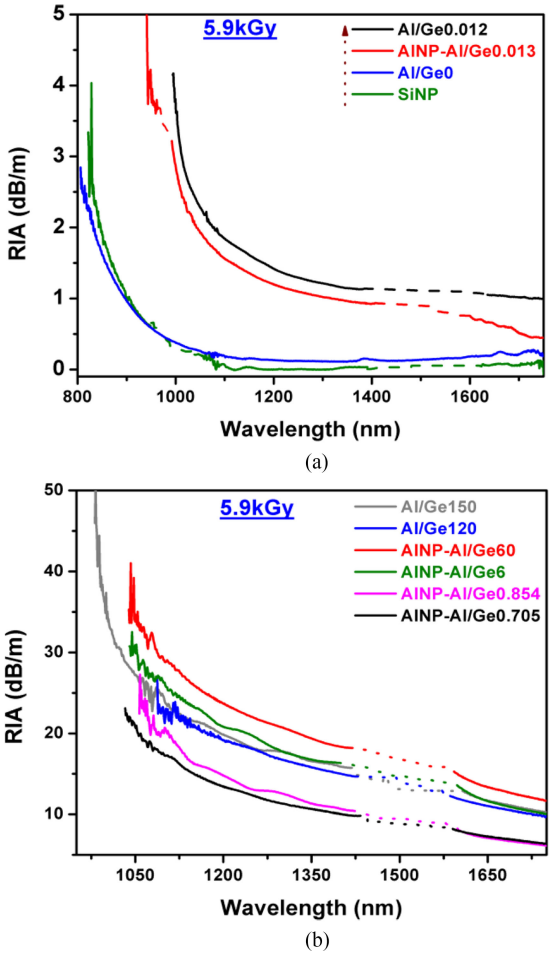

Fig. 1. RIA spectra of Er^{3+} doped germano-silica fibers (a) low content of Al/Ge ratio and (b) high content of Al/Ge ratio. The broken lines, interpret RIA interpolation in the Er^{3+} absorption bands.

In contrast, the RIA measurement was performed on the Al_2O_3 codoped germano-silica fiber such as AlNP-Al/Ge0.013 (Fig. 1(a)) that reveals higher RIA, when compared to the Al free and to a small quantity of Al doped fibers namely Al/Ge0 and SiNP fiber respectively. More precisely, the RIA of AlNP-Al/Ge0.013 fiber is increased by a factor of two in the investigated spectral range. This result confirms a negative impact of Al, although it is introduced in the form of Er-Al_2O_3 nanoparticles in the investigated fibers. However, it is important to underline that the AlNP-Al/Ge0.013 fiber exhibits a lower RIA as compared to a similar BEF (Al/Ge0.012) fiber. Therefore, the incorporation of Al ions in the form of Al_2O_3-nanoparticles seem to improve the radiation resistance when compared to the standard BEF fiber (Al/Ge0.012).

Fig. 1(b) illustrates the RIA spectra of high Al_2O_3 content doped (> 2.0 wt.%) Er^{3+}-germano-silica fibers and we focused here on a comparison between the NP and BEF fibers for various Al/Ge ratio ranging from 0.7 to 150. As shown in Fig. 1(b), the RIA of AlNP-Al/Ge0.705 and AlNP-Al/Ge0.854 fibers are found to be more or less similar where the erbium content is twice in the AlNP-Al/Ge0.854 fiber. However, it is worth noticing that RIA is ten orders of magnitude higher than that of Al-free fibers (Al/Ge0 and SiNP) and nearly seven orders of magnitude higher than Al-doped fibers (AlNP-Al/Ge0.013 and Al/Ge0.012) as reported in Fig. 1(a).

With increasing Al/Ge ratio by a factor of 6 (mostly small amount of Ge), we observed that AlNP-Al/Ge6 fiber shows a higher RIA with the same size of Er_2O_3-Al_2O_3 nanoparticles. Therefore, our experimental results demonstrate profoundly that the presence of a significant amount of Ge with Al_2O_3 (e.g., Al/Ge $\sim$ 1.0) could bring some benefits even if Al has been introduced in the form of Al_2O_3 nanoparticles.

Now, let us consider two BEF (Al/Ge120 and Al/Ge150) fibers with high Al_2O_3 content where the second one (Al/Ge150 fiber) has a much higher Er concentration (7 times higher). As it can be seen in Fig. 1(b)), there is no discrepancy in the RIA level of these two BEF fibers within the investigated spectral domain. These results demonstrate again no apparent impact of Er^{3+} on the RIA for such high Al/Ge ratio BEF fibers. In addition, the RIA of Al/Ge120 and Al/Ge150 fibers are found to be at the same level as AlNP-Al/Ge6 fiber, whereas their Al/Ge ratio is strongly unfavorable when the concentration of Al/Ge ratio is above 60. So here BEF technology appears better than NP one for such high Al content - low Ge content fibers. These observed positive results at high Al/Ge ratio may be due to the suppression of clustering formation, homogeneous dispersion and change in the coordination number of aluminum ion in the germano-silica fibers.

Finally the AlNP-Al/Ge60 fiber shows the highest RIA (see in Fig. 1(b)) among all investigated Er^{3+}-doped fibers. In particular, the RIA of this fiber is significantly higher than one of a similar fiber (AlNP-Al/Ge6) made with 25 nm Al_2O_3 nanoparticles. This result is likely due to the fact that we have much smaller Er-Al_2O_3 NP with a diameter $\sim$5 nm instead of 25 nm for all other AlNP based fibers and high Al/Ge ratio. To summarize, SiO_2 nanoparticles doped fiber is the most radiation resistant one against irradiation in the low Al content fiber category, whereas nanoparticle technology fibers with high Al-content are better than BEF fibers, which brings some benefits in terms of RIA if they have Al/Ge ratio around 1.0 and potentially even lower. For high Al content-high Al/Ge ratio, BEF technology remains better than NP.

C. *Defect Analysis: Electron Paramagnetic Resonance*

In order to investigate the creation of point defects, the electron paramagnetic resonance (EPR) measurements of germano-silica optical fibers were performed, before and after γ-irradiation. For non-irradiated fibers (0 kGy), they exhibit no signal which is below over the detection limit. The EPR spectra, on the other hand, of γ-irradiated germano-silica fibers exhibit a stronger and main resonance signal (Fig. 2(a) and (b)) at a g-factor of $\sim$2.0. The complex EPR spectra result from different signals are mainly due to the contribution of both Si- and Ge-related which paramagnetic point defects [22]–[27]. The main signal can be described with $g_1 = 2.00041$, $g_2 = 1.99997$ and $g_3 = 1.99264$ components which can be ascribed to the Ge(1) defect [22]–[26]. The universally accepted structure of Ge(1) is an electron trapped at a fourfold coordinated Ge atom; $(GeO_4)^-$

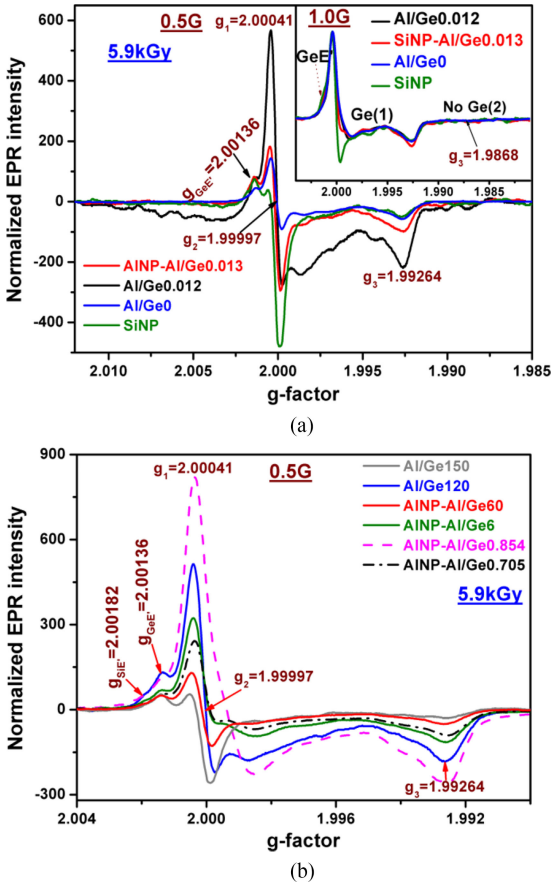

Fig. 2. EPR spectra of Er^{3+} doped germano-silica fibers at 1 mW, 0.5 G (a) low content of Al/Ge ratio. The inset of Fig. 2(a) shows the EPR spectra of fibers at 1 mW, 1.0 G and (b) high content of Al/Ge ratio.

[22]–[26]. The other signal with a weak component arising at g = 2.00136 is due to the GeE' centers. The corresponding microscopic structure of GeE' center is ≡Ge˙, a localized unpaired electron on a threefold coordinated Ge with different ligands [22]–[26]. In the present case, the $g_3 = 1.9868$ component of Ge(2) could not be detected in the γ-irradiated germano-silica fibers after γ-irradiation of 5.9 kGy, but it may be below the threshold limit of the EPR set up (see in the Fig. 2(a) inset) [22]–[26]. Moreover, similar measurement was repeated at 1 mW and 1.0 G (see in the inset of Fig. 2(a)). The line shape of our EPR spectra is in very good agreement with reported literature [22], [26], [28], [29].

As reported in Fig. 2(a), it can be seen that the EPR signal consists of both Ge(1) and GeE' centers in the Al/Ge0 fiber. On the contrary, more GeE' centers are visible with a very small amount of Ge(1) defect in the SiNP fiber.

In the case of Al-Er codoped fibers (Fig. 2(a)), AlNP-Al/Ge0.013 fiber exhibits high concentration of Ge(1) signals, whereas similar concentration of GeE' centers than SiNP and Al/Ge0 after γ-irradiation at the same dose. Therefore, Al_2O_3 could contribute to the generation of more Ge(1) defects significantly. Moreover, it is found that AlNP-Al/Ge0.013 fiber disclose lower defect concentration as compared to the BEF fiber: Al/Ge0.012. Therefore, less Ge(1) and GeE' are formed as a consequence of unambiguously SiO_2 and Al_2O_3 nanoparticles only. It is directly correlated with the RIA measurements.

Fig. 2(b) illustrates the EPR spectra of high Al-content fibers at around g = 2.0. We see that AlNP-Al/Ge0.854 shows a higher concentration of Ge(1) defects mainly in contrast to the AlNP-Al/Ge0.705 and AlNP-Al/Ge6 fibers. The huge increment in the AlNP-Al/Ge0.854 fiber may be taking place on account of the high hydroxyl groups. Therefore, the defect amplitude in the AlNP-Al/ Ge0.705 fiber is higher than in the AlNP-Al/Ge0.013 fiber even if the process is the same but there is a huge Ge difference. Notwithstanding, γ-ray radiation induces an extra small hump at g = 2.00182 in the EPR spectra which is a well-known characteristic of the SiE'_γ centers (O≡Si•) [5], [27], see in Fig. 2(b).

Let us consider the BEF fibers (Al/Ge120 and Al/Ge150), the Ge(1) defect number follow an opposite trend with the Al/Ge ratio (see in Fig. 2(b)). This is associated with the RIA measurement of Al/Ge120 and Al/Ge150 fibers. The weak SiE'_γ center is observed only for low content of germanium, while no SiE'_γ center is detected at high content of germanium at this condition (1.0 mW, 0.5 G).

From Fig. 2(b), it is interesting to observe that lower concentration of Ge(1) defect is found in AlNP-Al/Ge60 (NP-5nm). This result might be due to the fact that less specific surface i.e., the lower size of the Al_2O_3 nanoparticles, induces more accommodation of nanoparticles and an excess of the oxygen molecules [27]. Consequently, lower concentration of Ge(1) defects and at the same time leads to an increase of GeE' negative part (Fig. 2(b)). Thus, the experimental results suggest that the concentration of defects strongly relied on the size of the nanoparticles and codopants.

The EPR spectra displayed in Fig. 3(a) and (b) over a larger scale show a doublet signal which is characterized by a hyperfine parameter ($A_{iso} = 74$ G) attributing to the H (I) defect [11]. The H(I) doublet is caused by the hyperfine interaction between an unpaired electron spin (S = 1/2) of ^{29}Si and nuclear spin (I = 1/2) of the hydrogen atom in its nearest neighbour of the silica network [11]. We are not focusing on the analysis of NBOHC defect formation in the present study owing to this defect can be formed in both core and cladding of the fibers. Furthermore, neither AlOHC nor AlE' centers are identified at various power levels whatever optical fibers. This is mainly due to the presence of germanium and fiber drawing speed. On the contrary, to present fibers, we observed the formation of AlOHC and AlE' centers in the fiber preforms when the Ge content is less than 4.4 wt.% [28].

IV. Discussion

A. *Effect of Erbium Content*

A recent study of the RIA measurement was reported in the Er^{3+} doped silica fibers by Likhachev et al. that demonstrates a slightly higher RIA for fibers with a high Er_2O_3 content with the same GeO_2 concentration (15 mol.%) [2]. Moreover, they

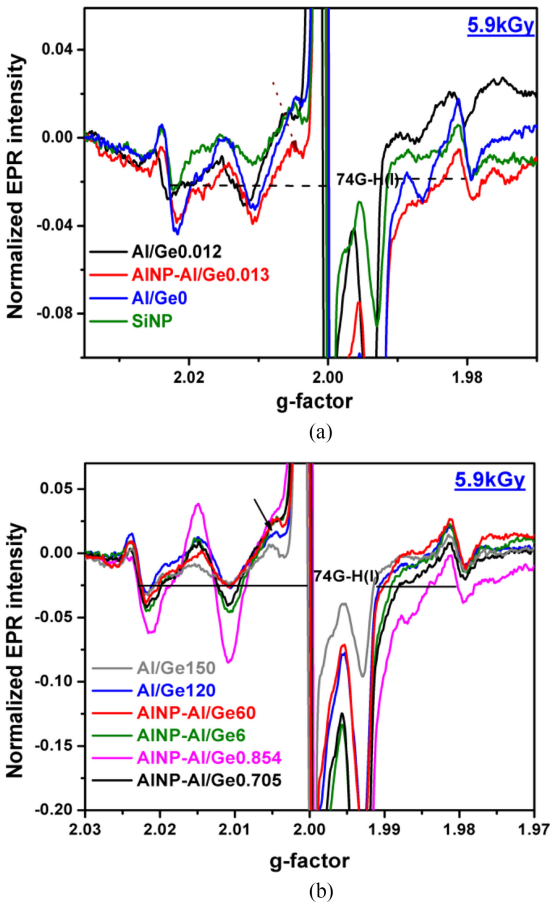

Fig. 3. EPR spectra of Er^{3+} doped germano-silica fibers at 1 mW, 3.0 G (a) low content of Al/Ge ratio and (b) high content of Al/Ge ratio.

also showed that RIA decreases with a small amount of GeO_2 (0.05 mol.%) at constant Al_2O_3 content (4.0 mol.%) [2]. In our study, the RIA is slightly higher when increasing Er^{3+} content in NP fiber type, but this variation appears negligible, according to the chemical composition variations associated to the GeO_2 or Al_2O_3 concentrations (Fig. 1(a) and (b)). Haruna *et al*., reported, based on the extend X-ray absorption fine structure (EXAFS) analysis, an increasing oxygen coordination number of Er^{3+} with Al-content and the Er-O bond distance enhanced as compared to the free of Al co-doping in fibers [1]. It was examined by Mebrouk *et al*. [12] that the photoreduction of Er^{3+} ions taken place in to Er^{2+} ions with accompanying Al-OHC and AlE' defect centers in the Er^{3+}-aluminosilicate and germano-silicate fibers at a lower dose of 300 krad based on the RIA method. We confirmed recently the photoreduction of Er^{3+} to Er^{2+} accompanied with the AlOHC defect formation and RIA increases with Er^{3+} concentration in sol-gel silica glasses after 5.9 kGy γ-irradiation dose [5]. It is interesting to note that Er^{2+} ion formation may be limited by the Er^{3+} ion in NP doped fiber preforms and optical fibers [28]. This is consistent with the absence of AlOHC even for low Ge content in Al/Ge120 and Al/Ge150 fibers as well. From EPR measurements, there is no significant variations recognized in both GeE' and Ge(1) defect concentrations, when the nanoparticles are incorporated into the fiber core.

B. Impact of Nanoparticle Technology

As it can be seen from Fig. 1(a), Er-SiO_2 and Er-Al_2O_3 nanoparticles doped fiber exhibit lowest RIA due to the lower concentration of Ge-, Si-, and suppression of Al-OHC defects as confirmed by the EPR results. It is a consequence that comes from the fact that these nanoparticles are embedded into the glass matrix. This leads to improve the Si-O and Ge-O bond strength and thus it is more difficult to break the strained bonds under ionizing radiation when compared to the standard fibers such as Al/Ge0 and Al/Ge0.012. In addition, there are less clustering in nanoparticles despite the presence of Al_2O_3 in the form of the NP.

After establishing EPR measurements, the formation of paramagnetic defect centers by irradiation have been revealed precisely, namely Ge(1), GeE', SiE', and H(I) centers (see in Figs. 2(a), (b) and 3(a), (b)). For Al/Ge0 fiber, the EPR spectrum reveals obviously the superposition of both GeE' and Ge(1) centers. As a comparison, SiNP fiber exhibits more GeE' centers, while the Ge(1) positive peak decreases dramatically and an increase in the negative peak of GeE' centers redundantly (see in Fig. 1(a), green color signal). On the other side, g_3 component of Ge(1) defect remains with the same amplitude in SiNP fiber as referred to the Al/Ge0 fiber. This represents the photo-bleaching of the germanium oxygen deficient centers-II (Ge-ODC(II)) in the SiNP fiber, which is strongly supported by the RIA study of SiNP fiber preform [28]. For fiber preforms, the Ge(2) signal features are detected at concentration of germanium typically higher than 22 wt.% [28]. In contrast, even if g_1 and g_2 components of the Ge(2) signal may be overlapped with Ge(1) and GeE' signal, the g_3 component $(g_3 = 1.9868)$ is completely absent of the EPR spectra in the fibers (Fig. 2(a), inset). Therefore, the experimental results allow us to conclude that there are no Ge(2) centers in the studied fibers. In fact, the concentration of Ge(1) and Ge(2) relied on the number of nearest neighboring germanium ions in the network [26] and fiber drawing conditions.

As it can be seen in Fig. 2(a), Al_2O_3 nanoparticles (AlNP) doped fiber generates more Ge(1) defect concentration compared to the SiNP and Al/Ge0 fiber. This result suggests that an enhancement of the perturbative role of Ge in the network [22]. For Al/Ge0.012 fiber, it is worthy to note that large concentration of Ge(1) defect centers is observed whereas lower concentrations in Al_2O_3 nanoparticles doped fibers.

The plausible mechanism for generation of GeE' and Ge(1) centers in the γ-irradiated Er^{3+} doped germano-silica fibers are included in the remark that defect population in optical fibers occurs mainly due to the cleavage of strained oxygen deficient centers (type-I) i.e., ≡Ge-R≡ (R = Ge, Si or Al) bonds in the Al doped germano-silica fibers through radiolysis process. It is usually admitted that GeE' centers formation takes place through radiolysis process route; $\equiv \text{Ge-Ge} \equiv +\gamma - \text{radiation} \rightarrow \text{GeE}' + \text{GeO}_3^+ + \text{e}^-$ [23], [29]. We assumed that another possibility might be occurring, the GeE' centers could originate from ≡Ge-O-Al strained bonds. This is more likely in high Al_2O_3 containing Er^{3+} doped germano-silica fibers (Al/Ge = 60, 120 and 150). The Ge(1) defect formation taken place from an electron transfer from bridging oxygen to

germanium in the GeO_4 tetrahedral units [29], [30]. Another pathway for the formation of Ge(1) defect centers is the radiative induced electrons coming from either oxygens or Al and both (O, Al) are likely being trapped on the substitutional four fold coordinated Ge atoms leading to Ge(1), as follows $GeO_4 + e^- \rightarrow (GeO_4)^\bullet$ [24].

Two fold-coordinated silicon (=Si or ODC-II) reacts with a neutral hydrogen atom (H_0) leading to the H(I) defect and their structure designated as $= Si^\bullet$-H other than germanium ($= Ge^\bullet$-H, H(II) defect) in the studied Er^{3+} doped nanoparticles germano-silica fibers (Fig. 3(a) and (b)) [11]. Our experimental features demonstrate the lower intensity of the H(I) defect signal in nanoparticles doping fibers in contrast to the BEF fibers.

C. Impact of Al/Ge Ratio on Ge and Si Related Defects

Although high content of Al_2O_3 ($\geq$3–4 wt.%) glasses and fibers under ionizing radiation show usually detrimental effects in term of higher RIA in the Vis-Near-IR range. However, Al is substantially useful for getting larger gain bandwidth and enhanced luminescence properties, and these are more important for the telecommunication applications. However, it appears here, that an increment in the RIA and gain degradation with Al_2O_3 content due to the fact that Al-related defects increase [5], [6]. This higher RIA could be partly compensated by codoping with germanium. Therefore, in the present case, the optimal Al/Ge doping ratio should be at around 1.0 (see in Fig. 1(b)) where the lowest RIA is observed in the fibers namely AlNP-Al/Ge0.705 and AlNP-Al/Ge0.854.

From Fig. 2(b), it is worthwhile to note that the concentration of GeE' and Ge(1) defects is amplified by an increasing Al/Ge ratio of 0.012 up to 150 in Er-Al_2O_3 (NP = 25 nm) nanoparticles and BEF fibers other than AlNP-Al/Ge0.854 fiber. These results indicate that the concentration of Ge(1) defects increasing with the Al/Ge ratio at certain concentration of Al/Ge = 120 and thereafter reverse trend was observed while the GeE' centers greatly enhanced. This can be attributed to change in the structure of germanium when high Al content. The high content of Al_2O_3 doped germano-silica fibers causes an increasing number of strained bonds inside the Ge-O-R (R = Ge, Si or Al) and more electrons captured by Ge from Al leading to the high concentration of GeE' centers taken place.

In Fig. 3(b), H(I) defect sensitivity decreases with increasing Al/Ge ratio in the form of Al_2O_3 nanoparticles and it depends on the size of the nanoparticles as well (for instance AlNP-Al/Ge6 (25 nm) and AlNP-Al/Ge60 (5 nm)).

D. Impact of Al/Ge Ratio on Al Related Defects

In optical fiber preforms, our previous results show that Al related centers are only observed with Ge concentration lower than 4.4 wt.% [28]. In particular, Al-E' centers are observed only in samples with Ge concentration lower than 4.4 wt.% independently of the NP technology, while AlOHC centers are only observed in the standard samples without nanoparticles [28]. However, in the present case, we do not detect any Al defects in optical fibers even if very high Al/Ge ratio of 120, 150 corresponding to Al/Ge120 and Al/Ge150 fibers respectively.

The lack of Al-E' centers could be due to the electron affinity of Er^{3+}, which compete with the AlO_3 centers as electron trapping centers and could prevent the formation of Al-E' centers, when the Er^{3+} concentration is high enough. Another possibility is that the fiber drawing process has reduced AlE' defects precursors.

The fiber drawing process can directly enforce an additional negative compressive stress on the fibers [31]–[33]. Thus, the net stress implying more population of the oxygen deficient centers (ODC(I) and ODC(II)) and larger flexibility in the fiber network resulting in the lack of Al-OHCs. Indeed, the high concentration of ODC(I) and ODC(II) could be the cause of the lack of AlOHC's, as oxygen hole centers compete with the AlOHC as hole-trappers and could prevent the formation of these centers when their concentration is high enough. According to the previous literature [34], they confirmed that aluminum ions in the silica network can produce principally AlO_6 octahedral and AlO_4 tetrahedra structural units. In our case, AlO_4 tetrahedral units could capture previously released/diffused oxygen atoms from the oxygen deficient centers ($\equiv$Si-Si$\equiv$) during fiber drawing giving more AlO_6 octahedral unit's formation. This may be an explanation for the lack of AlOHC in the present fibers after γ-irradiation.

V. Conclusion

In summary, the impact of a new SiO_2 and Al_2O_3 nanoparticle doping technology in term of RIA and defect formation in the Er^{3+}-doped germano-silica fibers were systematically investigated by using complimentary spectroscopic techniques. The experimental results reveal that the level of RIA in SiNP doped fiber is much lower than standard ones despite the presence of Al_2O_3 in the glass matrix. This is in agreement with Thomas *et al*. who reported that lowest gain degradation under γ-radiation occurred in the SiNP fibers [17], [18].

From RIA results in standard MCVD fibers, the optimization of the Al/Ge ratio in the studied fibers should be at around 1.0 wt.% implying a better performance in the nanoparticles doped optical fibers. However, for high Al content (>3.0 wt.%) – low Ge content fibers (<1.0 wt.%), BEF technology appears better than NP one.

Aluminum nanoparticles and high Al content−high Al/Ge ratio (Al/Ge = 120, 150) (BEF) fibers exhibit large concentration of GeE' centers. Therefore, it was concluded that the concentration of defects strongly dependent on the Al_2O_3 and on the size of the nanoparticles. The H(I) defect centers is observed, but there is no impact of hydroxyl groups on the Ge-related defects in the core (no H(II)).

Eventually, based on the RIA and EPR measurements compared to MCVD fibers, SiNP fiber is best one, in spite of it has low content of Al_2O_3. Our experimental results bring a new insight on the radiation resistance of SiO_2 and Al_2O_3 nanoparticles doped germano-silica fibers. This nanoparticles based doping technology is a significant way for improving the radiation resistance of erbium doped fiber amplifiers enabling their use in photonic sub-systems for satellite communications.

REFERENCES

[1] T. Haruna, J. Iihara, K. Yamaguchi, Y. Saito, S. Ishikawa, and M. Onishi, "Local structure analyses around Er^{3+} in Er-doped fiber with Al-codping, *Opt. Express*, vol. 14, no. 23, pp. 11036–11042, Nov. 2006.

[2] M. E. Likhachev *et al.*, "Radiation resistance of Er-doped silica fibers: effect of host glass composition," *J. Lightwave. Technol*, vol. 31, no. 5, pp. 749–755, Mar. 2013.

[3] T. S. Rose, D. Gunn, and G. C. Valley, "Gamma and proton radiation effects in erbium doped fiber amplifiers: Active and passive measurements," *J. Lightwave Technol.*, vol. 19, no. 12, pp. 1918–1923, Dec. 2001.

[4] E. J. Friebele *et al.*, "Erbium nanoparticles doped fibers for efficient, resonantly-pumped Er-doped fiber lasers," *Proc. SPIE*, vol. 9344, pp. 934412-1–934412-8, 2015.

[5] B. Hari Babu *et al.*, "Radiation hardening in sol-gel derived Er^{3+} doped silica glasses," *J. Appl. Phys.*, vol. 118, no. 12, pp. 123107-1–123107-7, Sep. 2015.

[6] S. Girad *et al.*, "Proton and gamma induced effects on erbium doped optical fibers," *IEEE Trans. Nucl. Sci.*, vol. 54, no. 6, pp. 2426–2434, Dec. 2007.

[7] G. M. Williams and E. J. Friebele, "Space radiation effects on erbium-doped fiber devices: Sources, amplifiers and passive measurements," *IEEE Trans. Nucl. Sci.* vol. 45, no. 3, pp. 399–404, Jun. 1998.

[8] S. Girard *et al.*, "Radiation hardening techniques for Er/Yb doped optical fibers and amplifiers for space application," *Opt. Express* vol. 20, no. 8, pp. 8457–8465, Apr. 2012.

[9] C. Fukuda, Y. Chigusa, T. Kashiwada, M. Onishi, H. Kanamori, and S. Okamoto, "γ-ray irradiation durability of erbium doped fibres," *Electron. Lett.*, vol. 30, no. 16, pp. 1342–1344, Aug. 1994.

[10] M. V. Uffelen, S. Girard, F. Goutaland, A. Gusarov, B. Brichard, and F. Berghmans, "Gamma radiation effects in Er-doped silica fibers," *IEEE Trans. Nucl. Sci.* vol. 51, no. 5, pp. 2763–2769, Oct. 2004.

[11] A. Morana *et al.*, "Influence of neutron and gamma-ray irradiations on rad-hard optical fibers," *Opt. Mater. Express*, vol. 5, no. 4, pp. 898–911, Apr. 2015.

[12] Y. Mebrouk, F. Mady, M. Benabdesselam, J.-B. Duchez, and W. Blanc, "Experimental evidence of Er^{3+} ion reduction in the radiation induced degradation of erbium-doped silica fibers," *Opt. Lett.*, vol. 39, no. 21, pp. 6154–6157, Nov. 2014.

[13] P. B. Lyons and L. D. Looney, "Enhanced radiation resistance of high-OH silica optical fibers," *Proc. SPIE*, vol. 1791, pp. 286–296, Feb. 1992.

[14] K. V. Zotov *et al.*, "Radiation resistant Er-doped fibers: Optimization of pump wavelength," *IEEE Photon. Technol. Lett.* vol. 20, no. 17, pp. 1476–1478, Sep. 2008.

[15] S. Girard *et al.*, "Radiation-hard erbium optical fiber and fiber amplifier for both low and high-dose space missions," *Opt. Lett.*, vol. 39, no. 9, pp. 2541–2544, May. 2014.

[16] F. L. Galeener, D. B. Kerwin, A. J. Miller, and J. C. Mikkelsen, Jr., "X-ray creation and activation of electron spin resonance in vitreous silica," *Phys. Rev. B*, vol. 47, no. 13, pp. 7760–7779, Apr. 1993.

[17] J. Thomas *et al.*, "Radiation-resistant erbium-doped-nanoparticles optical fiber for space applications," *Opt. Express*, vol. 20, no. 3, pp. 2435–2444, Jan. 2012.

[18] J. Thomas, "Impact de la nanostructuration des fibres dopées erbium sur leurs performances: Application aux contraintes du spatial," Thèse de Doctorat, Univ. Montpellier 2, Montpellier, France, Dec. 2013.

[19] H. Henschel, O. Köhn, and U. Weinand, "Radiation hardening of pure silica optical fibers by high pressure hydrogen treatment," *IEEE Trans. Nucl. Sci*, vol. 49, no. 3, pp. 1401–1409, Jun. 2002.

[20] H. Henschel, O. Kohn, H. U. Schmidt, J. Kirchhof, and S. Unger, "Radiation induced loss of rare earth doped silica fibers," *IEEE Trans. Nucl. Sci*, vol. 45, no. 3, pp. 1552–1557, Jun. 1998.

[21] I. Savelii *et al.*, "Nanostructuring an erbium local environment inside sol-gel silica glasses: Toward efficient erbium optical fiber lasers," *Laser Phys. Lett.*, vol. 13, no. 2, pp. 025108-1–025108-7, Jan. 2016.

[22] A. Alessi, S. Agnello, F. M. Gelardi, G. Messina, and M. Carpanese, "Influence of Ge doping level on the EPR signal of Ge(1), Ge(2) and E'Ge defects in Ge-doped silica," *J. Non-Cryst. Solids*, vol. 357, no. 8–9, pp. 1900–1903, Dec. 2011.

[23] S. Agnello *et al.*," Effect of oxygen deficiency on the radiation sensitivity of sol-gel Ge-doped amorphous SiO_2," *Eur. Phys. J. B*, vol. 61, no. 1, pp. 25–31, 2008.

[24] L. Giacomazzi, L. M. Samos, A. Boukenter, Y. Ouerdane, S. Girard, and N. Richard, "Ge(2), Ge(1) and GeE' centers in irradiated Ge-doped silica: a first-principles EPR study," *Opt. Mater. Express*, vol. 5, no. 5, pp. 1054–1064, May 2015.

[25] D. L. Griscom, "On the natures of radiation-induced point defects in GeO_2-SiO_2 glasses: Reevaluation of a 26-year-old ESR and optical data set," *Opt. Mater. Express*, vol. 1, no. 3, pp. 400–412, Jul. 2011.

[26] J. Nishii, K. Kintaka, H. Hosono, H. Kawazoe, M. Kato, and K.-I. Muta, "Pair generation of Ge electron centers and self-trapped hole centers in GeO_2-SiO_2 glasses by KrF excimer-laser irradiation," *Phys. Rev. B*, vol. 60, no. 10, pp. 7166–7169, Sep. 1999.

[27] G. Vaccaro *et al.*, "Structure of amorphous SiO2 nanoparticles probed through the E'γ centers," *J. Phys. Chem. C*, vol. 116, pp. 144–149, 2012.

[28] M. Leon *et al.*, "Influence of Al/Ge ratio on radiation-induced attenuation in nanostructured erbium-doped fiber preforms," presented at the Conf. Lasers and Electro-Optics: Science and Innovations, San Jose, CA, USA, 2015, Paper SM3L.8.

[29] H. Shigemura, Y. Kawamoto, J. Nishii, and M. Takahashi, "Ultraviolet-photosensitive effect of sol-gel derived GeO_2-SiO_2 glasses," *J. Appl. Phys.*, vol. 85, no. 7, pp. 3413–3418, Apr. 1999.

[30] J. Wen, G.-D. Peng, W. Luo, Z. Xiao, Z. Chen, and T. Wang, "Gamma irradiation effect on Rayleigh scattering in low water peak single mode optical fibers," *Opt. Express*, vol. 19, no. 23, pp. 23271–23278, Nov. 2011.

[31] P. L. Chu and T. Whitbread, "Measurements of stresses in optical fiber and preform," *Appl. Opt.*, vol. 21, no. 23, pp. 4241–4245, Dec. 1982.

[32] G. Origlio, M. Cannas, S. Girard, R. Boscaino, A. Boukenter, and Y. Ouerdane, "Influence of the drawing process on the defect generation in multistep-index germanium-doped optical fibers," *Opt. Lett.*, vol. 34, no. 15, pp. 2282–2284, Aug. 2009.

[33] S. Girard *et al.*, "Radiation effects on silica based preforms and optical fibers—I: Experimental study with canonical samples," *IEEE Trans. Nucl. Sci*, vol. 55, no. 6, pp. 3473–3482, Dec. 2008.

[34] S.-L. Lin and C.-S. Hwang, "Structures of CeO_2-Al_2O_3-SiO_2 glasses," *J. Non-Cryst. Solids* vol. 202, no. 1-2, pp. 61–67, Jul. 1996.

Author's biographies not available at the time of publication.